FLOW FRICTION AND HEAT AND MASS TRANSFER IN A SWIRLED FLOW

R. Z. Alimov

Inzhenerno-Fizicheskii Zhurnal, Vol. 10, No. 4, pp. 437–446, 1966

UDC 536.244+532.501.312

An experimental investigation has been made of flow friction and heat and mass transfer inside cylindrical tubes with exit sections without diaphragms and various degrees of swirl of one- and two-phase flows. A comparative analysis of the results obtained has been made. The most suitable operating conditions from the energy standpoint have been established for vortex heat and mass transfer equipment.

Experimental equipment and test method. A detailed account of this question has been given in [1, 2]. In order to obtain more general relationships, tests have since been performed with tubes of various sizes, and with varying degrees of swirl of the stream resulting from the use of swirl generators of various sizes with various numbers of tangential slits (see the table).

In the course of the experiments, besides calculation of mass flow rates of air and water, static pressure was measured both along the tube and at the entrance to the swirl generator in a section of the feed nozzle distant not less than five hydraulic diameters from the nearest rim of a tangential slit, in order to avoid appreciable local disturbances. Because of these considerations the total length of the nozzle was 25–30 hydraulic diameters. To obtain average values, the pressure in each section was measured at several points located uniformly along the perimeter. The excess pressure of the air supply to the vortex did not exceed $5 \cdot 10^4$ N/m^2. The tests spanned the range of Re numbers from $3 \cdot 10^2$ to $5 \cdot 10^5$.

Wall temperature was measured with chromel-kopel thermocouples at 2–3 points in each of 4–7 sections, depending on the tube size. Their readings were compared with those of a special thermocouple whose sensing head was embedded in the wall and whose leads had isothermal sections flush-mounted in grooves in the inner tube wall and fastened with a heat-resisting insulating cement made of talc chloride in waterglass, as well as with the readings of radiation and optical pyrometers in conditions where the temperature of the hottest end of the tube reached 600–900° C. We were thus able to assess the errors in temperature measurement arising from local disturbance of the flow by the hot thermocouples and from extraction of heat by the thermocouple leads.

In fabricating the thermocouples, thin wire of diameter 0.2–0.25 mm was mainly used; the sections of the wires near the hot junctions were carefully heat-insulated, depending on the temperature conditions and the tube diameter, with asbestos-glass wool or porcelain fiber; special attention was given to securing uniform size of the hot junctions and to locating them close to the wall, the installation being reckoned complete only when identical readings were obtained from all the thermocouples located at one section. Because of these precautions, the difference of temperatures measured by the various methods did not exceed 15–20% of the temperature head in the most unfavorable conditions, and during the investigation of mass transfer, because of the lower temperature level of the whole system, the readings of the two types of thermocouples practically coincided. Owing to the excessive technical difficulties (installation and suitable sealing), the thermocouples with the head embedded in the wall and the isothermal section were used only in isolated cases to estimate the errors.

Reduction of flow friction data. The simplified model of a swirling gas stream is a hollow rotating jet with a central core that is very weak in the kinematic and dynamic sense [3–7]. As it proceeds along the tube, the jet becomes gradually thicker because of attenuation of the swirl by friction forces. For an ideal stream swirling in a tube without diaphragms, according to a method described in [8] relating to centrifugal injectors, the following relations may be obtained:

$$\mu = \left[\sqrt{\frac{1}{\varphi^2} + \frac{A_\tau^2 (1 + \sqrt{1-\varphi})^2}{4(1-\varphi)}} \right]^{-1},$$

$$A_\tau^2 = \frac{8(1-\varphi)^2}{\varphi^3 (1 + \sqrt{1-\varphi})}; \qquad (1)$$

$$\zeta_\tau = 1/(A_\tau \mu)^2; \qquad (2)$$

$$s_r = 2\pi (1 - h/2) \operatorname{tg} \beta,$$

$$h = 1 - \sqrt{1-\varphi}, \quad \operatorname{tg} \beta = 1/A_\tau \varphi. \qquad (3)$$

Here $\zeta_\tau = \zeta_a + \zeta_t + \zeta_r$ is the theoretical value of the resistance coefficient of a vortex tube, indicating the magnitude of the total head on the scale of the inlet velocity head and expended in creating the axial ζ_a and tangential ζ_t components of velocity head, and the centrifugal pressure ζ_r, where

$$\zeta_t = 1, \quad \zeta_a = \operatorname{tg}\beta^2 \text{ and } \zeta_r = \frac{\int_0^h (\zeta_\tau - \operatorname{tg}\beta)\, y\,(2-y)\, dy}{h}. \qquad (4)$$

In the last expression, the law of distribution of centrifugal pressure over jet thickness in the form

$$\zeta_y = (\zeta_\tau - \operatorname{tg}\beta)\, y\,(2-y) \qquad (5)$$

was obtained from the equation of equilibrium of the swirling stream under conditions of potential distribution of tangential velocity, when the excess pressure at the inner edge of the stream is zero. The geometrical characteristic A_T in the relations presented

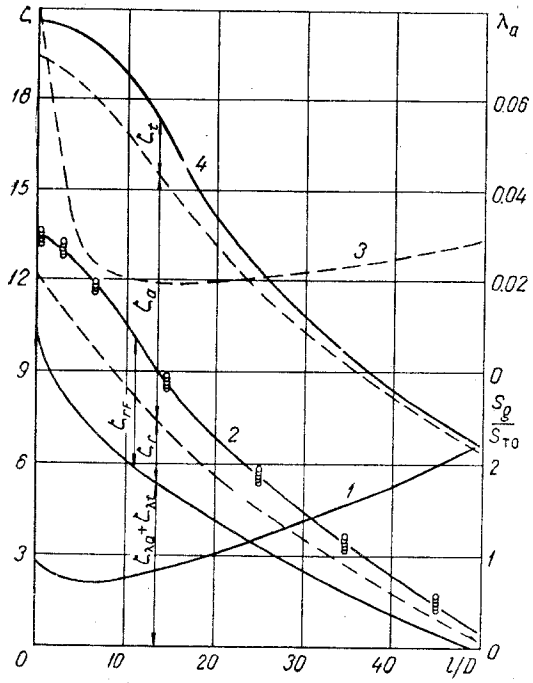

Fig. 1. Variation of the parameters of an isothermal swirling stream along a tube for the case $A_{T_0} = 0.43$: 1) s_g/s_{T_0}; 2) $\zeta_c = \zeta_{rF} + \zeta_{\lambda a} + \zeta_{\lambda t}$ (the points are experimental data); 3) λ_a; 4) $\zeta_g = \zeta_t + \zeta_a + \zeta_r + \zeta_{\lambda a} + \zeta_{\lambda t}$.

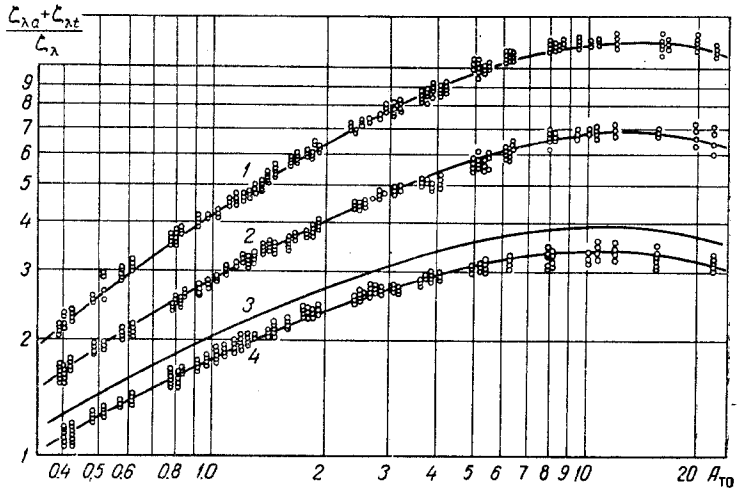

Fig. 2. Variation of the friction resistance ratio for swirling and axial streams as a function of geometrical characteristics: 1) with $l/D = 10$; 2) 20; 3) 40; 4) 50.

is defined as the ratio of the areas of the cross section of the tube and the longitudinal section of the jet, i.e.,

$$A_\tau = F_\tau / F_t. \quad (6)$$

For an ideal stream the quantity F_t coincides with the total section area of the tangential slits. For a real stream it varies along the tube. Representing the geometrical characteristic in the form (6) permits its use in the study of the laws of attenuation of a real stream.

In actual conditions attenuation of the swirl leads to change of the jet parameters along the tube. Therefore, for a viscous and nonisothermal stream, by dividing it into axial and tangential components, we can write the over-all resistance coefficient of a vortex tube with respect to the inlet velocity as follows:

$$\zeta_g = P_0/(\gamma_0 w_0^2/2g) = \zeta_{t0} + \zeta_{\lambda a} + \zeta_{\lambda t} + \zeta_{ia} + \zeta_{it}. \quad (7)$$

Here ζ_{t0} is the theoretical resistance coefficient of the vortex tube, according to [2], for the inlet section; $\zeta_{\lambda a} = \frac{1}{v_0 w_0^2} \int_0^l \frac{\lambda_a v w_a^2 dx_a}{D_{ra}}$ is the portion of the resistance coefficient due to friction of the axial flow component; $\zeta_{\lambda t} = \frac{1}{v_0 w_0^2} \int_0^l \frac{\lambda_t v w_t^2 dx_t}{D_{rt}}$ is the same for the tangential component; $\zeta_{ia} = \frac{2w_{ak}^2}{w_0^2}\left(\frac{v_k}{v_0} - 1\right)$ is the portion of the resistance coefficient due to acceleration as a result of the axial component being nonisothermal; $\zeta_{it} = \frac{2w_{tk}^2}{w_0^2}\left(\frac{v_k}{v_0} - 1\right)$ is the same for the tangential component.

By analogy with ordinary nonswirling flow, the last two terms have been represented in the form of twice the difference of the change due to heating in the velocity heads at the exit section [9]. In using (7), the exit velocity head is referred to the losses, but the inlet, outlet, and jet expansion losses, due to redistribution of the velocity field, will be included in the friction resistance coefficients.

The nature of the variation of the stream parameters along the tube, required for the calculations according to (7), was determined by means of a semiempirical method involving visual observation of the change of pitch of the jet, followed by calculation of all the remaining flow parameters (A_τ, φ, h, $\mathrm{tg}\,\beta$, w_a/w_0, w_t/w_0, D_{ra}, D_{rt}, etc.) with the aid of Eqs. (1)–(6) for any section and conditions, taken in dimensionless form for the sake of generality.

Visualization of the flow, mainly local, was accomplished in glass tubes by injecting very thin jets of water, or, in the case of large swirl velocities, jets of smoke, through special apertures, using hollow needles. We note that for the initial section of the tube, where attenuation is not as yet so strongly apparent, the measured values of the pitch s_g in the whole range of variation of A_T from 0.4 to 24 were very close to the theoretical values according to (3), independent of the Re number.

The values of the friction resistance coefficients λ_a and λ_t were determined using experimentally obtained graphs of static pressure variation along the wall. Here the assumption was made that the static pressure at any section is the sum of the centrifugal pressure, determined from (5) with y = h, and the drop due to flow friction at the tube wall. The numerical values of λ_a and λ_t were evaluated in each case by assuming $\lambda_t = 4c_f = \lambda_a$. Calculations of this kind were done for all the conditions investigated.

Figure 1 shows the relevant curves for $A_{T_0} = 0.43$ as an example. The nature of the change of pitch along the tube is also shown there, in addition to the variation of the remaining components of the resistance coefficient (ζ_a, ζ_t, and ζ_r). It should be noted that over most of the tube length λ_a remains less than for an axial stream with the same relative roughness. It was established, using an axial stream, that the relative roughness of the tubes investigated, including the glass tubes, lies in the range 0.0008–0.003, for which the mean value of λ in the turbulent region is approximately 0.03. The sharp increase of λ_a in the initial section is related with the effect of some decrease of pitch in comparison with s_T, and therefore, of some contraction of the swirling jet immediately after it enters the tube, this contraction being characteristic for the range of variation of A_{T_0} from 0.4 to roughly 2, i.e., for a relatively wide jet.* With increase of A_{T_0} the discontinuity in λ_a at the tube entrance gradually decreases, but its mean value for the whole tube increases smoothly at large A_{T_0}, approaching the axial flow value for a given roughness.

In the given stage of the investigations, embracing a comparatively narrow range of variation of $\bar{\Delta}$, we did not pursue a detailed study of the influence of this parameter on the hydrodynamic characteristics of a swirling stream. It is enough to remark that increase of roughness accelerates attenuation of the vortex, on the one hand, thus promoting decreased friction resistance, while, on the other hand, it increases λ_a and λ_t, causing greater resistance. These two opposing factors almost compensate one another. The result is, therefore, that the resultant value of the friction resistance in the test range of $\bar{\Delta}$ and Re in question is practically independent of these parameters. Moreover, no noticeable variation of friction resistance was observed, and this agrees with theory, within the investigated range of variation of slit length, width, and number for A_{T_0} = const. From the viewpoint of initial losses, however, the most favorable condition should be that where the slit length, or the total length of several slits, is equal to the pitch of the jet, for in that case the thickness of the latter will equal the thickness of the slit, and its entrance will

*The phenomenon is similar to common cases of contraction of a non-swirling jet (discharge from an orifice, flow over weirs, dams, etc. [10]).

not be accompanied by an appreciable alteration of cross section, and hence of velocity profile.

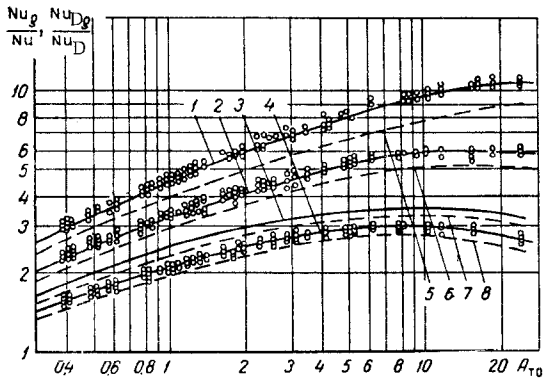

Fig. 3. Variation of Nusselt number ratio for swirling and axial streams as a function of the geometrical characteristic: 1, 2, 3, and 4) heat transfer with l/D of 10, 20, 40, and 50, respectively; 5, 6, 7, and 8) mass transfer with l/D of 10, 20, 40, and 50, respectively.

The most general results of the investigations are shown in Fig. 2. It is not difficult to establish that the predominant part of the loss of head due to flow friction occurs in the initial section of the tube, this becoming more distinct with increase of A_{T_0}. The curve of friction resistance as a function of A_{T_0} passes through a maximum, due to the increasing role of the streams. These graphs allow one to determine the friction resistance, and, in addition, by using (7), the total resistance for any vortex tubes in the investigated range of l/D and A_{T_0}.

The laws of variation of friction resistance coefficient with water injection, i.e., for two-phase flow, remain qualitatively the same as for single-phase flow. Two-phase flow is accompanied by formation of a liquid film on the inner wall of the tube, at moderate specific water flow rates, not exceeding 500–600 kg/m · hr, which occur in the overwhelming majority of mass transfer equipment of the film type and were obtained in the present tests. In practical calculations it is possible to neglect the comparatively small variation of resistance coefficient resulting from the diverse influence of many factors (variation of physical parameters due to the presence of the film, expenditure of power in swirling the liquid ejected by the action of the latter at low gas flow rates, etc.).

It should be noted that at appreciable velocities of a swirling stream, the two-phase regime is accompanied by uniform fluctuations of pressure, and by the appearance of annular waves [11] on the surface of the rotating liquid film.

Heat transfer data. In the heat transfer investigations the initial and final sections of the tube, of two calibers total length, which, as calibration tests showed, are appreciably influenced by the end losses, were not taken into account in the calculations. The residual working section had the dimensions shown in the table.

Analysis of the differential equations describing the process shows that the presence of centrifugal forces does not lead to the appearance of new similarity criteria [12, 13], except for the group A_T, which is the geometrical characteristic of the swirling stream. Therefore the generalized test data for constant values of A_{T_0} have been dealt with in the form of the dependence $Nu_g = f(Re)$. Analysis of these relations shows that all points relating to identical values of A_{T_0} and l/D lie, in the turbulent region, on a single straight line, parallel to that for the ordinary axial stream. In the transition region, the sharp fall in heat transfer typical for an internal problem is not observed, which is due, in all probability, to the stabilizing influence of the centrifugal forces, as well as to the fact that the swirling stream is a superposition of two flows—axial and tangential—differing appreciably as regards the location of the region in question.

The degree of variation of heat transfer in the turbulent region is very fully presented in Fig. 3. It may be seen that the swirl of the stream can actually be intensified by heat transfer, but its rate of growth with increase of A_{T_0} decreases, since the relatively thin jets corresponding to large values of A_{T_0} intensify the heat transfer in the initial section more strongly, and at the same time are attenuated more rapidly.

There is an interesting qualitative similarity between the graphs of relative growth of friction resistance and heat transfer in vortex tubes, indicating that it is possible to use the hydrodynamic analogy for analysis of flows as complex as the swirling stream. A certain quantitative lag in the rate of increase of friction at small A_{T_0}, and, on the other hand, a small lead at large A_{T_0}, are due in all probability to the growing influence of the centrifugal forces in intensifying heat transfer. We note that here, in contrast with the method usually adopted (see [14]) for comparison, the friction resistance of the entire tube is used, not the friction coefficient, a matter which is not at variance with the premises on which the hydrodynamic theory of heat transfer is based.

Calculation shows that, for identical values of the mean wall temperature t_w and heat flux q, a swirling stream may effect a considerable economy in the power expended in compressing the gas. As an example, Fig. 4 shows several graphs of the ratio of this power for axial and swirling streams as a function of A_{T_0}. The air mass flow rate to attain the given t_w and q was determined by simultaneous solution of the heat balance and heat transfer equations. The influence of the initial section for the axial stream was calculated according to [14]. The power required to drive the air was assumed proportional in both cases to the product of its volume flow rate and the total head at the tube entrance. The latter was determined for the swirling stream by means of (7). In this treatment the velocity head at the tube exit is also included in the total head developed by the compressor.

The graphs presented show that the greatest gain in power is achieved at comparatively small stream

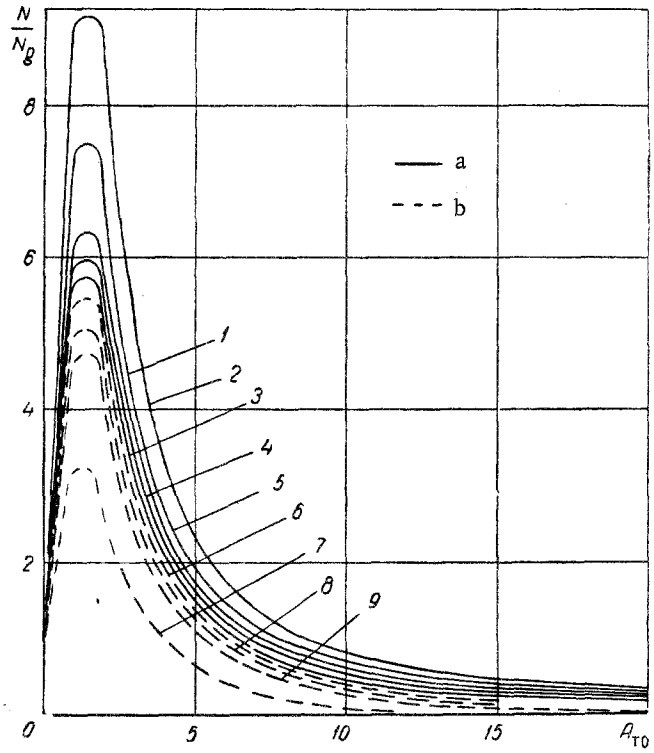

Fig. 4. Dependence of the ratio of power expended in compressing the air in axial and swirling motion on the geometrical characteristic for tubes with $l/D = 20$: a) for heat transfer [1) at $\phi = 67$ mm, $q = 75$ kW/m^2 and $t_w = 500°$ C; 2) 67, 75, and 250, respectively; 3) 15.6, 150, and 500; 4) 15.6, 150, and 250; 5) 15.6, 75, and 250]; b) for mass transfer with $g_l = 100–200$ kg/m · hr [6) at $\phi = 67$ mm, $g_\beta = 11.5$ kg/m^2 · hr, $q_\beta = 75$ kW/m^2 and $t_F = 60°$ C; 7) 15.6, 11.5, 75, and 60, respectively; 8) 15.6, 23, 150, and 60; 9) 15.6, 11.5, 75, and 40].

Dimensions (in mm) of Vortex Tubes and Number of Slits in Vortex Generators

ϕ 15.6		ϕ 22.4		ϕ 40	ϕ 67	ϕ 202
l/D = 10, 20, 40, 50		10, 20, 40, 50		10, 20, 40	10, 20	10
a×b×n	a×b×n	a×b×n	a×b×n	a×b×n	a×b×n	a×b×n
0.8×10×1	2×40×2	1.2×40×1	4×40×1	6×75×1	2.5×73×1	10×190×1
0.8×10×2	2×50×1	1.2×40×2	4×40×2	6×75×2	2.5×73×2	10×190×2
1.2×10×1	2×50×2	2×19×1	4×45×1	8×43×1	4×72×1	20×186×2
1.2×10×2	2.8×26×1	2×19×2	4×45×2	8×43×2	4×72×2	20×186×1
1.2×25×1	2.8×26×4	2×40×1	4×45×4	20×80×1	8×70×1	70×160×1
1.2×25×2	4×26×1	2×40×2	8×30×1	20×80×2	8×70×2	70×160×2
2×19×1	4×26×2	4×26×1	8×30×2	—	10×70×1	—
2×19×2	6×30×1	4×26×2	8×44×1	—	10×70×2	—
2×26×1	6×30×2	4×26×3	8×44×2	—	10×70×3	—
2×26×2	8×30×1	4×26×4*)	11×42×1	—	10×135×1	—
2×40×1	8×30×2	4×40×2*)	11×42×2	—	10×135×2	—

*Both slits on the one side.

swirl in the A_{T_0} range roughly from 0.4 to 4. The gain increases with increase of tube diameter and heat flux, and with decrease of mean wall temperature, and is quite appreciable in absolute value. For the same expenditure of power, the swirling stream will achieve more intense heat transfer, but because of the more rapid increase of power than of heat transfer as the gas flow rate increases, the gain under this method of comparison will be considerably less than the values of Fig. 4 would indicate.

Mass transfer data. The mass transfer investigation was conducted at the surface of the water film, the thin, continuous layer covering the inner surface of a vortex tube heated from the outside. The thermal power was increased up to the limit of the electric heaters and reached 200 kW/m^2 in individual cases.

The mass transfer test data were correlated in terms of similarity criteria in the form of the relation [1]

$$\mathrm{Nu}_{Dg} = f(\mathrm{Re},\ p_B/p_{\Gamma M}). \qquad (8)$$

With this treatment, within the limits of accuracy of the experiments, estimated to be of the order of 15–20%, the dependence of the degree of intensification of mass transfer on A_{T_0} proves to be qualitatively similar to the heat transfer process. The numerical results for the lower limit of liquid flow rate, 100–200 kg/m · hr, starting with which continuous films were created, taking into account evaporation over the whole internal surface under all the conditions investigated, are shown in Fig. 3 by the broken curves 5–8, obtained by appropriate mathematical reduction of the test data.* Further increase of the liquid mass flow rate leads to reduced mass transfer. Thus, at the highest liquid flow rate, equal to 500–600 kg/m × × hr, the mass transfer coefficient decreases by 20–25% on the average. The chief cause of the lesser intensification of mass transfer in comparison with heat transfer, as the liquid flow rate increases, is the motion of the film under the influence of the gas jet, leading to reduction of their relative velocity, and therefore to reduction in the mass transfer coefficient.

Figure 4 shows several curves relating to the mass transfer case, and a comparison was made for constant values of mean temperature of film t_F and evaporating liquid stream g_β. The air flow rate to attain the given t_F and g_β was calculated by simultaneous solution of the equations of mass balance and mass transfer. The power required to compress the air was determined in a manner similar to the heat transfer case. It may be seen that from the energy viewpoint the most appropriate region of variation of A_{T_0} remains roughly within the same limits as for heat transfer. Here the degree of gain increases with increase of tube diameter and of heat and mass flux, and with reduction of mean film temperature.

*For convenience of correlation, it was assumed that at large mass flux values, the mass transfer equation for axial flow [15] must also depend on the parameter $p_B/p_{\Gamma M}$ to the power 0.33.

NOTATION

R, D, l, and F_T – radius, diameter, length, and cross-sectional area of tube; a, b, and n – width, length, and number of tangential slits; $\varphi = F_a/F_T$, $h = H/R$, $s = S/R$, A_T, and β-effective cross-section coefficient, relative thickness, relative pitch, geometric characteristic, and angle of inclination of swirling jet; $D_\Gamma = 4F/U$, F and U – hydraulic diameter, cross-sectional area, and wetted perimeter of flow components; γ, v, and w – specific weight, volume, and mean mass velocity of air; $\bar{\Delta}$ – relative roughness; P_0 – total pressure at swirler inlet; Re – Reynolds number, based on tube diameter and gas flow rate; λ – friction resistance coefficient; ζ – resistance coefficients and total resistance component scaled to inlet velocity head; Nu and Nu_D – Nusselt thermal and diffusion numbers; t_w and t_F – mean integral wall and film temperature along tube; q and q_β – heat flux, and the portion of it expended on evaporation of the liquid; q_β – mass flux; p_B and $p_{\Gamma M}$ – total pressure of gas mixture, and logarithmic mean inert gas pressure at film surface and in flow; N – power expended in compressing air; x – path length of swirling jet; y – thickness coordinate of jet calculated from its inner edge; subscripts 0, k, and F – parameters in the initial and final sections and at the wall; a, t, r, and c – parameters of the axial, tangential, and radial flow components, and of the static pressure; g – test-derived parameters of swirling stream.

REFERENCES

1. R. Z. Alimov, Izv. AN SSSR, OTN, Energetika i avtomatika, no. 1, 1962.

2. R. Z. Alimov, collection: Heat and Mass Transfer [in Russian], 2, Izd. AN BSSR, Minsk, 1967.

3. Yu. V. Ivanov, B. D. Katsnel'son, and V. A. Pavlov, collection: Aerodynamic and Heat Transfer

Aspects of Boiler Furnaces, ed. G. F. Knorre [in Russian], GEI, 1958.

4. D. N. Lyakhovskii, collection: Aerodynamic and Heat Transfer Aspects of Boiler Furnaces, ed. G. F. Knorre [in Russian], GEI, 1958.

5. E. A. Nakhapetyan, collection: Aerodynamic and Heat Transfer Aspects of Boiler Furnaces, ed. G. F. Knorre [in Russian], GEI, 1958.

6. V. S. Martynovskii and A. M. Voitko, Teploenergetika, no. 2, 1961.

7. M. J. Sibulkin, Journ. Fluid Mech., **12**, no. 2, 1962.

8. G. N. Abramovich, Applied Gas Dynamics [in Russian], GITTL, 1953.

9. W. M. Kays and A. L. London, Compact Heat Exchangers [Russian translation], GEI, 1962.

10. R. R. Chugaev, Hydraulics [in Russian], GEI, 1962.

11. R. Z. Alimov, DAN SSSR, **157**, no. 6, 1964.

12. G. N. Delyagin, Tr. In-ta goryuchikh iskopaemykh, **19**, 24, 1962.

13. V. K. Shchukin, Tr. Kazanskogo aviatsionnogo in-ta, **26**, no. 76, 1963.

14. M. A. Mikheev, Fundamentals of Heat Transfer [in Russian], GEI, 1956.

15. L. D. Berman, Evaporative Cooling of Circulating Water [in Russian], GEI, 1957.

19 June 1965

Kazan Aviation Institute